Published in final edited form as:
J Nucl Med. 2009 October ; 50(10): 1655–1665. doi:10.2967/jnumed.108.055780.

^{18}F-FDG PET/CT for Image-Guided and Intensity-Modulated Radiotherapy*

Eric C. Ford[1], **Joseph Herman**[1], **Ellen Yorke**[2], and **Richard L. Wahl**[3]

[1]Department of Radiation Oncology and Molecular Radiation Sciences, Johns Hopkins University, Baltimore, Maryland [2]Department of Medical Physics, Memorial Sloan-Kettering Cancer Center, New York, New York [3]Russell H. Morgan Department of Radiology and Radiological Sciences, Johns Hopkins University, Baltimore, Maryland

Abstract

Advances in technology have allowed extremely precise control of radiation dose delivery and localization within a patient. The ability to confidently delineate target tumor boundaries, however, has lagged behind. ^{18}F-FDG PET/CT, with its ability to distinguish metabolically active disease from normal tissue, may provide a partial solution to this problem. Here we review the current applications of ^{18}F-FDG PET/CT in a variety of disease sites, including non–small cell lung cancer, head and neck cancer, and pancreatic adenocarcinoma. This review focuses on the use of ^{18}F-FDG PET/CT to aid in planning radiotherapy and the associated benefits and challenges. We also briefly consider novel radiopharmaceuticals that are beginning to be used in the context of radiotherapy planning.

Keywords

radiation therapy; IMRT; IGRT; FDG (fluorodeoxyglucose); FDG PET/CT

The tools of modern radiotherapy allow one to control with increasing precision where within a patient a radiation dose is deposited, the intent of which is to irradiate tumor tissue (and areas at high risk of locoregional metastases) while sparing nearby normal tissue. Intensity-modulated radiotherapy (IMRT) is currently the most advanced technology available for photons (1–3). IMRT finely tailors dose distributions by exploiting the many more degrees of freedom that are possible with spatial intensity modulation than with more traditional 3-dimensional conformal radiotherapy approaches. Using IMRT in head and neck cases, for example, the radiation oncologist can deliver concave dose distributions that treat large regions of the neck wrapping around the spinal cord and yet can limit the spinal cord itself to receiving a relatively low dose, thus minimizing cord damage (2). Also possible are spatially restricted dose distributions that treat tumors in the lung while sparing normal lung and heart, tumors in the brain while avoiding optic nerves and optic chiasm, or tumors in the prostate while sparing the adjacent rectum and bladder (3–7). Several implementations of IMRT are readily available as commercial products (8), and under development are improved approaches such as volumetric arcs, treatments in which the whole volume of tumor is treated with a continuous sweep of the gantry around the patient in one or multiple arcs (9,10).

*Note: For CE Credit, You Can Access this Activity through the SNM Web Site (http://www.snm.org/ce_online) through October 2010.

For correspondence or reprints contact: Eric C. Ford, Department of Radiation Oncology and Molecular Radiation Sciences, Johns Hopkins University, 401 N. Broadway, Suite 1440, Baltimore, MD 21231. eric.ford@jhmi.edu.

No potential conflict of interest relevant to this article was reported.

Coupled with these advances in dose delivery are new ways of localizing the patient's tumor and normal tissues during treatment. Although traditional methods rely on laser-based alignment of skin marks supplemented by periodic orthogonal radiographs, a modern radiotherapy clinic can be equipped with stereoscopic kilovoltage radiography capabilities or integrated CT guidance that allows precise alignment of patients with respect to the treatment beam (8,11,12). Monitoring patient position and dynamic changes during treatment is also possible with various technologies now available (13–15). This general paradigm of actively using imaging during treatment is referred to as image-guided radiotherapy. Through it, one can approximately halve the residual localization error of the structure defined as the target in the treatment-planning process, as determined with repeated imaging (16). Obviously, the degree to which localization error can be reduced depends on the site being treated, with intracranial tumors representing what is probably a best-case scenario, and a worse case being one with much motion and difficult visualization, such as a gastrointestinal site.

Even with all this technology to precisely control the delivery of a radiation dose, one is still left with the fundamental problem of determining what region of tissue needs to be targeted. This aspect of designing radiotherapy is often the most challenging. Interobserver variability using CT scans is well appreciated and documented for a variety of common disease sites, including cancer of the lung (17,18) and cancer of the head and neck (19,20), and is caused by difficulty in determining the exact boundary of a tumor, even for expert observers with the best CT protocols. Without an accurate delineation of the tumor region in the first place, precise control of dose distributions may not provide much additional tumor control.

PET scans with the radiotracer ^{18}F-FDG may be most useful in this regard. In many common cancers, PET with ^{18}F-FDG, or combined with CT, has greater sensitivity and specificity for disease detection than does CT or MRI alone (21). With its ability to distinguish metabolically active disease, ^{18}F-FDG PET/CT can provide important adjunctive information in designing a treatment plan. Figure 1 shows an example case for a patient with pancreatic cancer. In this case, a radiation oncologist has outlined the tumor region based on CT (yellow) and a nuclear medicine physician has outlined the tumor based on ^{18}F-FDG PET/CT (blue). The addition of ^{18}F-FDG PET/CT provides clear evidence of disease extending some 2 cm inferior to the boundary delineated by CT alone. Although there can be modest misregistrations between PET and CT due to breathing motion (22), this separation between the two regions reflects a real difference between apparent tumor locations on the 2 studies.

The present paper focuses on the use of ^{18}F-FDG PET/ CT to improve target definition in IMRT planning. Of course, this represents only one way in which ^{18}F-FDG PET is used in managing the care of cancer patients. Other uses of ^{18}F-FDG PET include better staging of disease to determine whether curative radiotherapy is suitable (23,24) and measurement of treatment response for further management as used in a variety of disease sites (25–28). Although most cancers are ^{18}F-FDG–avid, some—such as mucinous cancers of the colon, stomach, and other locations—may be less so. Thus, regions for treatment should be drawn with knowledge of the untreated tumor's avidity for ^{18}F-FDG. This review focuses on disease sites in which tumors are ^{18}F-FDG–avid and for which ^{18}F-FDG PET/CT is currently being most widely used for IMRT planning. We begin with a discussion of several physical imaging issues that apply to nearly all uses of this technology and then discuss each disease site separately.

Physical Issues

Delineation of Tumor Boundaries

One key advantage of ^{18}F-FDG PET in radiotherapy planning is its potential for improving tumor boundary delineation. ^{18}F-FDG PET may offer a better indication of the actual extent

of disease and may also reduce interobserver variability, thus making treatment volumes more standard over a wide range of physicians and centers, a concept that has been investigated by several authors (17,19,20,29,30).

The need for robust delineation of tumor boundaries becomes even more important in treatment schemes that deliver a dose in relatively few, high-dose (10–30 Gy) fractions, such as stereotactic body radiotherapy, which is being developed to treat the lung (31) and pancreas (32), among other sites. With high-dose schemes, smaller margins are used around the tumor to spare surrounding normal tissue. When smaller margins are used, however, there is less room for error. If the actual tumor is not delineated appropriately, it will fall outside the high-dose volume. In a standard fractionation approach (e.g., 30 fractions of 2 Gy each), large margins of approximately 1 cm are used around the tumor. A standard definition (International Commission on Radiation Units and Measurements, ICRU50) consists of a gross tumor volume (GTV) that is the radiologically appreciable tumor extent, expanded to a clinical target volume to account for microscopic extension, and finally to a planning target volume (PTV) to account for various physical uncertainties such as motion during treatment or day-to-day variability in tissue positions. In high-dose schemes, localization is strict and a GTV-to-PTV margin of only a few millimeters is used; for example, 2–3 mm would be used for stereotactic body radiotherapy of the pancreas (33) or 5 mm axially for the lung (31). With such strict localization, one must be confident of the accuracy of delineation, and ^{18}F-FDG PET/CT can have an important role in this regard. One must also pay close attention to the technical quality of the PET/CT scan to minimize potential misregistration between the PET and CT images, which are acquired sequentially and not simultaneously. One aspect of this is respiratory motion.

In the delineation of tumor boundaries using ^{18}F-FDG PET, there are several physical imaging issues that likely apply to all treatment sites (34). Foremost is the delineation method itself. There are two challenges to overcome here. The first has to do with the spatial resolution of the PET image, which as used in clinical practice is 7–9 mm after reconstruction with many systems. Even if the distribution of cancer cells were to abruptly end at some location, it would be challenging to identify this edge in the ^{18}F-FDG image given that partial-volume effects will blur the edges. Thus, deriving 1-mm boundaries from a technique with an intrinsically much lower resolution is not expected to be successful. PET excels at identifying the presence of tumor but can fall short at determining the precise margins.

Nevertheless, for the purposes of radiotherapy planning, some tumor edge must be delineated. The challenge is to identify the most appropriate method for delineation. The problem is illustrated in Figure 2, which shows ^{18}F-FDG PET/CT images from a patient with base-of-tongue cancer. If one uses a constant-threshold technique to delineate the boundary of the tumor, the volume of tumor returned will vary depending on the cutoff level that is chosen (Fig. 2B). An equivalent way to state this is that the tumor boundary will depend on the window and level setting chosen at the time of delineation, a point that has often been made.

This is not a small effect. As shown in Figure 3, the volume returned can vary by a factor of 2 or more depending on what level is chosen (35). Lesions smaller than approximately 5 cm^3 appear to be particularly sensitive to threshold changes because of the stronger influence of partial-volume effects for smaller tumors (see the 2 curves at the right in Fig. 3). Furthermore, delineation can also be affected by the PET reconstruction algorithm used, the filter size, and other physical parameters, which may not be well controlled (36,37). The relative activity level of the tumor and the background also clearly affects delineation, especially below source-to-background ratios of approximately 5 (37). These effects have been validated on phantoms in controlled situations (35,37–39). Approaches in which a percentage of a maximum value is used to define the edge of the lesion may be quite reproducible among varying operators, but it must be realized that varying implementations of the “maximum” value are in place. The

maximum standardized uptake value (SUV) or counts in an approximately 1-cm^2 region of interest is typically lower than that in the one maximum voxel (28). Because the PTV often extends a centimeter or more beyond the GTV, this effect may not be as large clinically as it might initially appear, however. The precise edge definition from PET remains challenging.

^{18}F-FDG–based delineation of tumor boundaries is thus problematic. There have been some attempts to address this issue and try to bring some standards to bear. One early study used phantoms of a known size in an attempt to define a standard threshold cutoff in ^{18}F-FDG PET voxel values that would return the proper object size (40). This study suggested that the threshold be set at 42% of the maximum uptake, though the study considered only lesions in the size range of 0.4–5.5 cm^3, a range in which threshold levels are extremely sensitive (Fig. 3). Another early approach that showed excellent accuracy in lung cancer size delineation was to determine the normal tissue activity in the healthy lungs and the variance. Tumor volume was selected as a region of ^{18}F-FDG avidity corresponding to tumor whose uptake was over 3 SDs above the normal lung background. This selection resulted in a generally excellent delineation of tumor and a good correlation of tumor size on CT and PET for untreated lung cancers (41). However, this approach works best with large tumors with high ^{18}F-FDG uptake in areas of low background activity. The appropriate background choice and number of deviations above that background appear to be tissue-specific.

In addition to these reports from the late 1990s, numerous studies have examined other delineation methods, including the use of different threshold values (36,39,42–47), the possibility of using a set SUV for the threshold (34,36), the use of iterative algorithms that take background into account (36–38), and the possibility of gradient detection techniques as an alternate approach to threshold contouring (48). Some studies simply ignored all the above effects and had treating physicians contour while using the window and level setting that they found most appropriate (45,49). It is reasonable to have a nuclear medicine physician or radiologist involved in each case for tumor delineation (34), especially since the formal training that radiation oncologists receive on PET is typically limited.

With all these technical issues still unresolved, it is unclear how targets should best be delineated. One possibly fruitful direction for resolving the controversies is to systematically correlate ^{18}F-FDG distributions with pathologic specimens, either in the form of gross tissue blocks from resection or needle biopsies. Some studies have attempted to do this. An early study by Wong et al. comparing ^{18}F-FDG PET, MRI, and CT in squamous cell carcinoma of the head and neck incorporated histopathologic data via identification of anatomic landmarks (50). Daisne et al. did a similar study with a much more detailed examination of surgical specimens from 9 patients who had total laryngectomies after imaging sessions with ^{18}F-FDG PET, CT, and MRI (51). Frozen sections were coregistered slice-by-slice using a system of wooden rods; the resulting volumetric reconstruction was registered with each of the imaging modalities. Results indicate that ^{18}F-FDG PET is the imaging modality delineating contours that are the closest to the actual specimen, though they are, on average, somewhat larger. CT and MRI volumes are significantly larger yet. Regions of nonoverlap were quantified, and on average, 13% of the pathologically suspect region was not included by PET because of extralaryngeal extension. Stroom et al. reported a similar study on non–small cell lung cancer (NSCLC) patients who underwent CT and ^{18}F-FDG PET before lobectomy (52). As with the laryngeal study, both CT- and ^{18}F-FDG PET–derived volumes were larger than pathologic specimens when deformations were considered. The report of van Baardwijk et al. (29) on NSCLC indicates the opposite. The diameter of resection specimens was somewhat smaller than that derived from autocontouring ^{18}F-FDG PET images. As more such validation studies are performed, the extent to which ^{18}F-FDG PET describes actual tumor extension in different disease sites will become more clear.

Given all the ambiguities in delineation, it is at present uncertain how to best incorporate ^{18}F-FDG PET/CT for IMRT planning as it relates to precise definition of the lesion margin. Clearly, additional lesions (which might not have been identified as abnormal on CT alone) can be identified by PET and PET/CT and can then be delineated by combination of the CT with the PET. In addition, in some instances, there is clear extension of the PET abnormality beyond the region seen on CT, as in the example case shown in Figure 1. Because the slope of the lesion edges on PET is quite sharp in many instances, it is probable that a typical margin of 1 cm beyond the lesion itself is adequate for standard use. Precise 1- to 2-mm delineation of the true edge of a tumor on PET, which has an 8-mm reconstructed resolution, is not expected to be successful. Thus, some extension beyond the visible PET margins typically needs to be applied.

Registration of Images

The advent of PET/CT scanners obviated the registration and display of PET and CT images from separate studies (53). Given that all PET scanners sold today are of the combined PET/CT type, the registration issue receives little consideration. One registration issue that does need to be considered, even with PET/CT technology, arises from the fact that the CT scan is obtained over a short time while the PET scan is obtained over a long time. Misregistration can result, as, for example, with breathing artifacts. Image registration can also become an issue for radiotherapy applications because the PET/CT scan is often acquired separately from the radiotherapy-planning CT scan, which has the special features of laser localization, a flat tabletop to simulate the treatment conditions, and customized devices to facilitate reproducible positioning of the patient. In principle, the PET/CT scan could be repeated, after staging and workup, with the patient in the treatment position. In practice, however, this is problematic because, although the first PET/CT scan is reimbursable for the staging of many sites (NSCLC, lymphoma, head and neck cancer, esophageal cancer, melanoma, and colorectal cancer), a second scan so soon afterward usually cannot be reimbursed (54). Image registration may therefore be required to align the PET/CT scan with the radiotherapy CT scan, with all the associated difficulties (39). This practical consideration has greatly limited the utility of ^{18}F-FDG PET/CT for radiotherapy.

Artifacts from Respiration

A special class of artifacts important in the radiotherapy context comes from the respiratory motion of the patient during the PET/CT study. It is well appreciated that respiratory motion can have a strong effect on the inferred activity distribution in ^{18}F-FDG PET (55). Using a snapshot with a fast CT scan, as opposed to older breathing-averaged transmission scans, can result in artifactual mislocalization of lesions (56). Cohade et al. (22) compared the location of lung lesions in 244 patients on PET versus CT from PET/ CT. They measured an average mislocalization of 7.6 mm, likely due to respiratory differences between the two scans. A more recent analysis of 216 lung cancer patients quantified the effect of using different CT scans for attenuation correction and the resulting impact on the inferred distribution of ^{18}F-FDG (57). For small lesions (<50 cm^3), the effects were largest, and when this group (n = 93) was divided according to the distance from the diaphragm, the mean mislocation of the GTV centroid ranged from 1.0 to 2.4 mm depending on how close the lesion was to the dome of the diaphragm, whereas the mean GTV volume changed by 16%–154% on average. Respiratory motion is expected to affect the delineation of tumors in the abdomen as well as in the lung. The degree of misregistration appears to be greater in the abdomen than, for example, in the bone in preliminary observations.

With the advent of respiration-correlated CT (4-dimensional CT) 5 years ago (58,59), it became possible to measure the motion of tumors. This same approach has been used to create 4-dimensional PET (60), which can use the 4-dimensional CT scan for attenuation correction.

Early studies with PET showed that if respiration can be controlled or compensated for (via respiratory gating, for example), then the effects of motion in PET images can be largely removed (55). The maximum lesion SUV is often increased, as the activity is not spatially smeared by breathing motion. Unfortunately, commercial solutions are not yet sufficiently well developed to be used routinely (54). Repeated breath-holds have been shown to reduce or eliminate breathing artifacts for diagnostic PET scans in patients who can comply (61,62). Breath-hold PET studies, however, are probably not relevant for most radiotherapy-planning purposes, since treatment needs to duplicate the conditions of the imaging study from which the target is defined: breath-hold imaging would have to be followed by breath-hold treatment at the same level of inspiration. Four-dimensional PET could be used to plan free-breathing radiotherapy under free-breathing conditions. If respiratory gating is used for treatment, the gate window would have to be defined around the appropriate imaging reference phase. If neither 4-dimensional PET/gating nor breath-hold treatment is possible, appropriate target margins must be designed.

Lung

Radiotherapy of NSCLC presents a difficult technical challenge. There is much evidence that, at conventional fractionation, doses above 70 Gy are necessary for local control (63). Because of respiratory tumor motion and general setup error, the treatment dose must be delivered to a PTV that is significantly larger than the GTV if breathing motion is anticipated. Traditional GTV-to-PTV margins in the lung are 1–2 cm. Normal lung and spinal cord are the major dose-limiting organs, and both have tolerance doses for potentially lethal toxicities that are far below 70 Gy. Treatment-planning studies show that IMRT can often escalate target dose while maintaining acceptable levels of predicted normal-tissue toxicity (6,64). Despite reservations in the literature about degradation of IMRT target coverage due to respiratory motion, and potential lung toxicity from increased lung volumes receiving low (10–20 Gy) doses (65), neither of these effects is a necessary consequence of IMRT lung treatment (66–68). And at least 2 single-institution studies have shown encouraging outcomes for such treatments (69, 70).

For T1 and small T2 tumors, there is growing evidence of surprisingly good local control by a new technique, stereotactic body radiotherapy (71,72). This method uses extreme hypofractionation schedules (e.g., 20 Gy × 3 fractions or 12 Gy × 4 fractions (71)) together with strict target localization during treatment, which therefore allows for tight (~0.5 cm) target margins. Compression is often used to restrict respiratory motion. Although IMRT may be used, most stereotactic body radiotherapy protocols achieve the desired dose distributions by using multiple (~10), conformally shaped noncoplanar beams. Increasingly, target localization involves in-room image guidance. The treatment plans are designed so that the high-dose region conforms tightly to the PTV, thereby protecting surrounding normal tissues. Although the biologic mechanisms are incompletely understood and could depend, for example, on mechanisms such as vascular damage at high doses, with 2- to 3-y median follow-up local control is competitive with surgery—far better than with even high doses at conventional fractionation—and the incidence of normal-tissue toxicity is low.

Accurate target definition is vital if these two delivery methods are to reach their full potential. Because ^{18}F-FDG PET is significantly superior to CT in sensitivity and specificity for diagnosis and staging of NSCLC (73), there is hope that ^{18}F-FDG PET will also lead to more accurately defined GTVs. Numerous studies show that, for NSCLC, target volumes defined by a combination of PET and CT (GTV_{PET+CT}) differ from those defined by CT alone (GTV_{CT}) regardless of whether the planning CT and the PET study are registered by software or by eye (44,49,74–77); these and others are cited in recent reviews (78,79). A Radiation Therapy Oncology Group (RTOG) protocol (RTOG 0515) with the primary objective of studying the

effect of PET/CT fusion on 3-dimensional conformal radiotherapy plans closed this year. The effect of respiratory motion is particularly important in lung cancer treatment. Even so, it has been suggested that a GTV defined with the aid of PET, including a lower threshold for segmentation, may map out the tumor's excursion and allow delineation of an internal target volume (80).

With the inclusion of ^{18}F-FDG PET, both increased and decreased tumor volumes have been observed. GTV_{PET+CT} is greater than GTV_{CT} if, for example, the main effect of PET is inclusion of a lymph node that was not apparent on the planning CT scan (49,79); in such a case, PET can prevent a geographic miss or can lead to a change in management. For example, stereotactic body radiotherapy, in its current form, is not appropriate for patients with mediastinal lymph nodes. GTV_{PET+CT} is less than GTV_{CT} if the lack of PET activity allows the physician to exclude a region of atelectasis from the GTV. In this case, it is easier to deliver a high target dose while satisfying the normal-tissue constraints. However, care is needed, as there is no pathologic confirmation that these regions are sufficiently tumor-free (79) or will receive enough incidental radiation to prevent recurrence even if they are not explicitly within the GTV.

^{18}F-FDG PET may improve interobserver consistency in target definition (17), especially if accompanied by computerized image registration (30). However, it is unclear whether PET truly improves the accuracy of target definition for NSCLC. Simple threshold-based segmentation methods (e.g., including in the PET GTV any voxel with SUV > 2.5, including any voxel with SUV > 40% of the lesion maximum, or using other percentage maximum SUV thresholds) have been shown to yield volumes that differ greatly according to the threshold. When the tumor is visible on CT, these can lead to either over- or under-coverage (36,79). Some tissue-correlative studies have appeared for NSLC (29,52) but much more work is required.

An often-cited strength of ^{18}F-FDG PET is the inclusion in the GTV of mediastinal nodes that might otherwise be missed (49,74,79) and the appropriate exclusion, without invasive procedures, of nodes without disease (81). Meta-analysis indicates that PET is more sensitive and specific than CT for mediastinal staging of NSCLC (24). However, ^{18}F-FDG PET nodal targets do not always agree with pathology (49,82), although the extent of disagreement has still not been ascertained. PET cannot detect microscopic disease, and PET often fails to detect disease that is less than 5 mm in diameter (83). Imaging later after injection may be advantageous, presumably because of more favorable pharmacokinetics at later times but still at a time when the ^{18}F-FDG activity is high (79). ^{18}F-FDG PET is being used to judge mediastinal involvement and is required as part of the RTOG protocol (RTOG 0236) for stereotactic body radiotherapy of stage I and II NSLC for staging and to eliminate hilar lymph node involvement. It is encouraging that one study (81) found that, with a minimum of 2 y of follow-up, only 6 of 57 patients treated with stereotactic body radiotherapy who were node-negative as assessed with ^{18}F-FDG PET had first failure in the nodes.

In summary, at present ^{18}F-FDG PET must be used cautiously in determining the target for lung cancer treatment. Although ^{18}F-FDG PET is excellent in identifying tumor-involved areas and in excluding bulk tumor from other areas, robust automatic segmentation methods are currently not available on commercial treatment-planning or PET workstations. There is imperfect agreement, whether the comparison is with a phantom, CT-visible tumors, or (unfortunately rarely) pathology. All these approaches have challenges, even direct tissue comparison, since fixation in formalin causes tumor deformation. Segmentation by an experienced radiation oncologist, with input from an expert at identifying all foci of ^{18}F-FDG–avid tumor on PET/CT (and ^{18}F-FDG–containing normal tissues), remains the best choice. Modern delivery techniques—especially aided by image guidance and respiration control—

can deliver a high dose to the prescribed volume. But ensuring that this volume includes the complete clinical target volume without excess normal tissue, even with the use of ^{18}F-FDG PET, remains a problem.

Head and Neck

Head and neck cancer was one of the earliest disease sites to which IMRT was applied, and the technique has been particularly beneficial here (2,84). IMRT can deliver complex dose distributions with multiple dose levels for different risk regions and, with its high dose gradients, can spare critical structures near the site of disease. One widely used application is parotid gland sparing to preserve salivary function, a common toxicity of radiotherapy for these diseases (85). With this highly precise means of delivering radiation dose comes the concomitant need for the often-difficult accurate delineation of the intended region of interest for IMRT planning (84). Though less well established than its use in lung cancer IMRT planning, ^{18}F-FDG PET may also be useful in delineating disease in head and neck cancers. The initial results with ^{18}F-FDG PET have appeared promising in terms of locoregional recurrence, but study sizes have been relatively small and follow-up short (86–90). Caution must be taken, since there are case reports of recurrences in regions that, on the basis of ^{18}F-FDG PET indications, were not irradiated (91).

The main utility of ^{18}F-FDG PET for head and neck cancer appears to be in distinguishing metastatic nodal disease for inclusion in the IMRT planning. Several studies have shown that ^{18}F-FDG PET has a high sensitivity for identifying nodes, often exceeding 90% and generally better than CT alone (92). One correlative pathology study found a 96% sensitivity for identifying diseased nodes—a sensitivity that was significantly better than the 78% available with CT alone (93). Using ^{18}F-FDG PET/CT to include lymph nodes that are equivocal on CT can have a beneficial impact on radiotherapy planning. The decision of whether to designate a node as positive for disease often translates into the difference between delivering a high radiation dose applicable for gross disease (e.g., 70 Gy) and delivering a prophylactic dose for at-risk nodes (e.g., 58.1 Gy) (94). The importance of this is underscored by the recent report of Sanguineti et al. (94) on 50 patients with oropharyngeal squamous cell carcinoma, which found that 50% of locoregional failures occurred as a result of nodes that were not identified on CT and were treated with only a lower prophylactic dose.

Several studies have examined the use of ^{18}F-FDG PET for identifying cancerous lymph nodes in the context of radiotherapy planning. Nishioka et al. found 39 nodes with ^{18}F-FDG PET/CT in 21 patients where only 28 would have been found by CT alone (87). This changed gross tumor delineation in 4 patients. Wang et al. (86) found that ^{18}F-FDG PET upstaged disease in 57% of patients (n = 28). Six patients had nodes that would not have been included in the gross disease volume on the basis of CT alone. Similarly, Scarfone et al. (45) cited at least one example patient in whom a diseased node was identified only on ^{18}F-FDG PET. Given the high resolution of modern CT scanners, however, the benefit of ^{18}F-FDG PET in nodal identification may be less marked than these studies suggest.

In the above use scenario, ^{18}F-FDG PET increases the volume of gross disease by the inclusion of more nodes with known disease. The alternative is a situation in which the size of the gross disease region is smaller with ^{18}F-FDG PET. This situation could occur for several reasons; for example, a necrotic node may appear negative on ^{18}F-FDG PET even though it harbors some residual disease. Such situations, in which ^{18}F-FDG–derived volumes are smaller, must be treated with extreme caution. Several studies have appeared in which the volume of identified disease decreased with the incorporation of ^{18}F-FDG PET in at least some cases: In a study by Ciernik et al. (39), 33% of cases (4/12) with a PTV decreased by more than 25%; in a study by Wang et al. (86), 44% of cases (7/16) had a smaller GTV on ^{18}F-FDG PET; and

in a study by Paulino et al. (47), 75% of cases (30/40) had a smaller GTV on ^{18}F-FDG PET. Similarly Daisne et al. reported that ^{18}F-FDG PET–derived volumes were significantly smaller than CT-derived volumes for pharyngolaryngeal squamous cell carcinoma (n = 29) (51). One counterexample is the 6-patient study of Scarfone et al. (45) in which all primary tumor volumes were larger on ^{18}F-FDG PET, though the volume was increased only by 15% on average. In summary, nearly all these reports showed numerous patients in whom the ^{18}F-FDG–derived tumor volume was smaller than the CT-derived tumor volume.

Using ^{18}F-FDG PET to shrink volumes is potentially dangerous. Though a smaller PTV can translate into improved normal-tissue sparing (87,95), it may also result in suboptimal local control. A report has appeared recently of 3 head-and-neck cancer patients who experienced locoregional recurrence after IMRT in the region of the spared parotid gland (91). In 2 patients, the failures were in periparotid lymph nodes that were deemed disease-negative on the basis of ^{18}F-FDG PET. In current practice, clinicians have a well-justified reluctance to reduce the size of the treatment volume in the head and neck on the basis of ^{18}F-FDG PET information.

One important potential advantage of including ^{18}F-FDG PET in the planning could be to reduce variability between users, thus making treatment volumes more standard over a wide range of physicians and centers. Although the inclusion of ^{18}F-FDG PET/CT does appear to reduce interobserver variability for lung tumors (17,29,30,96), it is not clear if such is true also for head and neck tumors. Two recent studies have examined this issue in head and neck cancer —one with 4 observers and 16 patients (19) and one with 8 observers and 10 patients (20). In both cases, the interobserver variability was actually somewhat worse with the inclusion of ^{18}F-FDG PET/CT. Though this appears to contradict the discussion above regarding the inclusion of PET, the effect may be because the technology is relatively new and institutional standardized protocols need to be implemented (19). The effect may also be due to the considerable complexity of glycolytically active anatomic structures in the head and neck, again supporting the need for inclusion of skilled PET/CT colleagues in the step of localizing ^{18}F-FDG–avid tumors and nearby ^{18}F-FDG–containing normal structures (97).

In all the above studies, there were physical imaging uncertainties that one must be aware of. In addition to the issues of tumor delineation method and artifacts, the head and neck are particularly affected by the problem of registering the PET/CT scan to the radiotherapy-planning CT scan. Because the neck is flexible, it may not be possible to register both the head and the lower neck between two studies if the flexion or extension is different. This is a recurrent theme in studies that examine ^{18}F-FDG PET for head and neck applications (45,86,87,95). To obviate this problem, some studies have recommended the use of standard rigid devices applied for patient immobilization in radiotherapy clinics, although this recommendation does require the prospective construction and use of these devices before the ^{18}F-FDG PET scan is acquired. Reimbursement issues make this solution problematic even in radiation oncology departments with PET/CT simulators. Other studies have used nonrigid registration to handle this problem, though such algorithms are not routinely available in most software (95).

Given all the above challenges, it is perhaps not surprising that there is no consensus on how or even whether ^{18}F-FDG PET/CT should be used in IMRT planning for head and neck cancer. Clinical examination and CT remain the de facto standard. ^{18}F-FDG PET/CT for target definition remains under investigation, but its utility may ultimately lie in its potential for identifying recurrence early (>6 wk) after IMRT treatment (92). PET may also be used to guide a radiation boost dose to hypermetabolic regions, an approach that is discussed in more detail below as it applies to newer tracers of tumor hypoxia.

Brain

The use of ^{18}F-FDG PET/CT for IMRT of brain tumors is even less well established, likely because the high background levels of surrounding gray matter often prevent brain tumors from being visualized well on ^{18}F-FDG PET alone (98). The situation may be improved by delaying imaging until up to 8 h after injection (99) or by using amino acid–based compounds (100) or tracers of proliferative activity (101). In the meantime, ^{18}F-FDG PET is unlikely to see widespread use for this disease site. Nevertheless, a few pilot studies have appeared. Tralins et al. used ^{18}F-FDG PET to delineate glioma tumor boundaries for a 20-Gy IMRT boost treatment beyond the standard dose of 59.4 Gy (102). The use of ^{18}F-FDG PET resulted in volumes that were unique beyond those found with MRI alone. Follow-up studies, however, showed that neither overall survival nor progression-free survival was improved with the ^{18}F-FDG–based boost irradiation (103).

Pancreas

Although pancreatic cancer is the ninth most common malignancy, it remains the fifth leading cause of cancer deaths in the United States, because most patients present with advanced disease at diagnosis (104). Stereotactic body radiotherapy has recently been implemented to treat the tumor plus a small margin (2–3 mm) to account for potential misalignment of the patient with respect to the treatment beam and for possible tissue motion during treatment (33,105). Although hypofractionated stereotactic body radiotherapy may be more convenient for patients (1–5 d of treatment, compared with 25 conventional treatments), there appears to be more treatment-related toxicity, which can lead to duodenal perforation in some cases (33). For stereotactic body radiotherapy, it is imperative that we be able to differentiate the pancreatic tumor from normal duodenum and small bowel—a challenge that ^{18}F-FDG PET can help address.

Only a few studies have included the use of ^{18}F-FDG PET/CT for defining pancreatic tumor regions (33), and it is unclear what the effect of adding ^{18}F-FDG PET will be. Though pancreatic tumors appear to be ^{18}F-FDG–avid, false-positive findings are possible in cystic tumors. Pilot investigations by 3 of the authors have indicated that ^{18}F-FDG PET/CT may be particularly useful in distinguishing tumor volume from the duodenum. Though it is obvious that the duodenum is adjacent to the pancreas, it is often difficult to visualize the exact boundary between the duodenum and the tumor even for an expert observer. An example is shown in Figure 4, where the target volume delineated on CT alone (yellow) extends much more inferiorly than the target volume delineated on ^{18}F-FDG PET/CT (blue). This is in contradistinction to Figure 1, in which the ^{18}F-FDG–avid region extends below that identified on CT alone. In contrast, in Figure 4, the ^{18}F-FDG PET scan indicates that the tumor border is more superior than that visualized on CT alone. Distinguishing the duodenal border may be particularly important given that duodenal toxicity has been encountered in early trials using stereotactic body radiotherapy. Though the best method for delineating tumor boundaries is still uncertain, the deviations noted here are gross and are unlikely to be affected by the exact delineation method.

Partial Breast Irradiation

^{18}F-FDG PET/CT may also find a use in the planning of partial breast irradiation. The goal of partial breast irradiation is to deliver a therapeutic radiation dose to the lumpectomy bed (target) and surrounding tissue only. There is widespread interest in this technique, and it is the subject of an ongoing trial from the RTOG/National Surgical Adjuvant Breast and Bowel Project (106). A fundamental challenge in partial breast irradiation is the accurate delineation of the lumpectomy bed, which is often difficult to distinguish on CT alone. Our group has investigated the use of ^{18}F-FDG PET/CT for this purpose (107). This is a somewhat novel use for the tracer,

in that the uptake is likely not associated with residual tumor but is instead a result of the postsurgical inflammatory process. Nevertheless, it is possible in most cases to distinguish the lumpectomy bed clearly on ^{18}F-FDG PET/CT. The ^{18}F-FDG PET–derived volumes tend to be larger than the volumes derived from CT alone, but an investigation of the radiation dosimetry consequences indicates that even with the larger ^{18}F-FDG PET–derived volume the dose contributions to normal tissue structures such as lung and heart remain acceptably low (107).

Other Radiopharmaceuticals

All the applications discussed here use, implicitly, the ^{18}F-FDG radiotracer. Though widely used for the practical reason that it is presently the single most effective tumor-imaging agent for PET across a wide range of cancers, ^{18}F-FDG traces a non–tumor-specific process, that is, the early steps of glycolysis. In general, ^{18}F-FDG uptake is related to the number of cancer cells that are positive for glucose transporter 1 (108,109). ^{18}F-FDG uptake is only modestly related to the proliferative rate of cancers, though this can vary (110). Increased ^{18}F-FDG uptake can be caused in an infectious or inflammatory response related to the accumulation of macrophages or polymorphonuclear leukocytes, which can efficiently sequester ^{18}F-FDG. Indeed in both animal models and humans, ^{18}F-FDG has proven to be a good tracer for detecting infections (111). Thus, uptake in nonmalignant processes is well recognized for ^{18}F-FDG. At the microscopic level, ^{18}F-FDG uptake has also been positively correlated with increased hypoxia and generally correlated with perfusion in direct comparative human studies using the ^{15}O tracer (112), and similar findings have been reported from NSCLC patient data in which SUVs from ^{18}F-FDG PET correlated with hypoxia-inducible factor 1α and glucose transporter 1 levels. Some studies have shown no differences in proliferation as measured by Ki67 levels (109), whereas other studies have (113,114). The relationship to hypoxia-inducible factor 1α is also somewhat variable.

These data and others like them indicate that many complex phenomena underlie an increase in ^{18}F-FDG uptake, despite the fact that it is a useful downstream marker of tumor location and viability. These mechanistic limitations have created great interest in using more specific radiotracers, and many of these are applicable to radiotherapy. There are, of course, many tracers specific to various molecular activities such as hypoxia or apoptosis. The reader is referred elsewhere for more complete overviews (115,116). To take a few examples, however, radiolabeled amino-acid tracers such as ^{11}C-methyl-methionine may be a more specific measure of metabolism that is less affected by inflammatory response and may therefore be especially useful for follow-up studies after radiotherapy (117), though they are not immune from such effects. Other specific probes include thymidine analogs such as 3′-deoxy-3′-^{18}F-fluorothymidine, which act as tracers of proliferation (118), or radiotracers such as ^{11}C-choline, which target the active phospholipid metabolism in tumors (119). For neuroendocrine tumors or thyroid cancer, more specific ligands are available.

The clinical deployment of novel radiotracers is in evolution, and it remains to be seen how the resulting PET or SPECT data will be used for radiotherapy applications. One example application is the use of a radiotracer such as ^{18}F-misonidazole to identify regions of the tumor that are hypoxic and therefore thought to be radioresistant. Once the hypoxic subregions are identified, an IMRT plan can be generated to deliver a higher boost dose to these regions (120). Such an approach, however, requires that the hypoxic regions be stable over the several-day timescale over which radiotherapy is delivered. Recent data with repeated ^{18}F-misonidazole PET scans on patients with head and neck cancer, however, indicate that these regions may not be stable (121). Hypoxia-derived boost radiation may still be possible but would have a smaller impact than it might if these regions were stable (122). A wide range of hypoxia-imaging agents is under study, and it remains unclear which, if any, will contribute beneficially to tumor imaging and treatment planning with PET/CT.

Conclusion

Radiotherapy planning has traditionally relied heavily on CT. Increasingly, ^{18}F-FDG PET/CT is also being incorporated into the treatment-planning process and promises to improve the ability to confidently identify regions of disease. Though there are numerous technical and biologic challenges to deploying ^{18}F-FDG PET for these purposes, it is in fairly common use at least for most of the disease sites discussed in this article. As radiation oncology moves toward hypofractionated stereotactic body radiotherapy for many sites, the role of ^{18}F-FDG PET will continue to evolve and provide additional benefit. It should also be recognized that although it appears obvious that the superior tumor detection capability of PET and its superior specificity for excluding tumor should translate into better patient outcomes, we lack comparative randomized trials in which PET is used, or not used, in the planning process. Such studies, though difficult, would be of great interest as the use of PET/CT expands into more applications based on its superb diagnostic performance.

References

1. Bortfeld T. IMRT: a review and preview. Phys Med Biol 2006;51:R363–R379. [PubMed: 16790913]
2. Boyer AL, Geis P, Grant W, Carol M. Modulated beam conformal therapy for head and neck tumors. Int J Radiat Oncol Biol Phys 1997;39:227–236. [PubMed: 9300758]
3. Ling CC, Burman C, Chui CS, et al. Conformal radiation treatment of prostate cancer using inversely-planned intensity-modulated photon beams produced with dynamic multileaf collimation. Int J Radiat Oncol Biol Phys 1996;35:721–730. [PubMed: 8690638]
4. Murshed H, Liu HH, Liao Z, Barker JL, Wang X, Tucker SL, et al. Dose and volume reduction for normal lung using intensity-modulated radiotherapy for advanced-stage non-small-cell lung cancer. Int J Radiat Oncol Biol Phys 2004;58:1258–1267. [PubMed: 15001271]
5. Khoo VS, Oldham M, Adams EJ, Bedford JL, Webb S, Brada M. Comparison of intensity-modulated tomotherapy with stereotactically guided conformal radiotherapy for brain tumors. Int J Radiat Oncol Biol Phys 1999;45:415–425. [PubMed: 10487565]
6. Liu HH, Wang X, Dong L, et al. Feasibility of sparing lung and other thoracic structures with intensity-modulated radiotherapy for non-small-cell lung cancer. Int J Radiat Oncol Biol Phys 2004;58:1268–1279. [PubMed: 15001272]
7. Ten Haken RK, Lawrence TS. The clinical application of intensity-modulated radiation therapy. Semin Radiat Oncol 2006;16:224–231. [PubMed: 17010905]
8. Mackie TR, Holmes T, Swerdloff S, et al. Tomotherapy: a new concept for the delivery of dynamic conformal radiotherapy. Med Phys 1993;20:1709–1719. [PubMed: 8309444]
9. Yu CX, Li XA, Ma L, et al. Clinical implementation of intensity-modulated arc therapy. Int J Radiat Oncol Biol Phys 2002;53:453–463. [PubMed: 12023150]
10. Otto K. Volumetric modulated arc therapy: IMRT in a single gantry arc. Med Phys 2008;35:310–317. [PubMed: 18293586]
11. Jaffray DA, Siewerdsen JH. Cone-beam computed tomography with a flat-panel imager: initial performance characterization. Med Phys 2000;27:1311–1323. [PubMed: 10902561]
12. Pouliot J, Bani-Hashemi A, Chen Josephine, et al. Low-dose megavoltage cone-beam CT for radiation therapy. Int J Radiat Oncol Biol Phys 2005;61:552–560. [PubMed: 15736320]
13. Balter JM, Wright JN, Newell LJ, et al. Accuracy of a wireless localization system for radiotherapy. Int J Radiat Oncol Biol Phys 2005;61:933–937. [PubMed: 15708277]
14. Ho AK, Fu D, Cotrutz C, et al. A study of the accuracy of cyberknife spinal radiosurgery using skeletal structure tracking. Neurosurgery 2007;60(2 suppl 1):ONS147–ONS156. [PubMed: 17297377]
15. Keall PJ, Kini VR, Vedam SS, Mohan R. Motion adaptive x-ray therapy: a feasibility study. Phys Med Biol 2001;46:1–10. [PubMed: 11197664]
16. Mageras GS, Mechalakos J. Planning in the IGRT context: closing the loop. Semin Radiat Oncol 2007;17:268–277. [PubMed: 17903704]

17. Caldwell CB, Mah K, Ung YC, et al. Observer variation in contouring gross tumor volume in patients with poorly defined non-small-cell lung tumors on CT: the impact of ^{18}FDG-hybrid PET fusion. Int J Radiat Oncol Biol Phys 2001;51:923–931. [PubMed: 11704312]
18. Giraud P, Elles S, Helfre S, et al. Conformal radiotherapy for lung cancer: different delineation of the gross tumor volume (GTV) by radiologists and radiation oncologists. Radiother Oncol 2002;62:27–36. [PubMed: 11830310]
19. Riegel AC, Berson AM, Destian S, et al. Variability of gross tumor volume delineation in head-and-neck cancer using CT and PET/CT fusion. Int J Radiat Oncol Biol Phys 2006;65:726–732. [PubMed: 16626888]
20. Breen SL, Publicover J, De Silva S, et al. Intraobserver and interobserver variability in GTV delineation on FDG-PET-CT images of head and neck cancers. Int J Radiat Oncol Biol Phys 2007;68:763–770. [PubMed: 17379435]
21. Wahl, RL.; Wagner, HN., Jr, editors. Principles and Practice of PET and PET/CT. 2nd. Philadelphia, PA: Lippincott Williams & Wilkins; 2008.
22. Cohade C, Osman M, Marshall LT, Wahl RL. PET-CT: accuracy of PET and CT spatial registration of lung lesions. Eur J Nucl Med Mol Imaging 2003;30:721–726. [PubMed: 12612809]
23. Fletcher JW, Djulbegovic B, Soares HP, et al. Recommendations on the use of ^{18}F-FDG PET in oncology. J Nucl Med 2008;49:480–508. [PubMed: 18287273]
24. Dwamena BA, Sonnad SS, Angobaldo JO, Wahl RL. Metastases from non-small cell lung cancer: mediastinal staging in the 1990s—meta-analytic comparison of PET and CT. Radiology 1999;213:530–536. [PubMed: 10551237]
25. Yao M, Graham MM, Smith RB, et al. Value of FDG PET in assessment of treatment response and surveillance in head-and-neck cancer patients after intensity modulated radiation treatment: a preliminary report. Int J Radiat Oncol Biol Phys 2004;60:1410–1418. [PubMed: 15590172]
26. Mac Manus MP, Hicks RJ, Matthews JP, et al. Positron emission tomography is superior to computed tomography scanning for response-assessment after radical radiotherapy or chemoradiotherapy in patients with non-small-cell lung cancer. J Clin Oncol 2003;21:1285–1292. [PubMed: 12663716]
27. Shankar LK, Hoffman JM, Bacharach S, et al. Consensus recommendations for the use of ^{18}F-FDG PET as an indicator of therapeutic response in patients in national cancer institute trials. J Nucl Med 2006;47:1059–1066. [PubMed: 16741317]
28. Wahl RL, Zasadny K, Helvie M, Hutchins GD, Weber B, Cody R. Metabolic monitoring of breast cancer chemohormonotherapy using positron emission tomography: initial evaluation. J Clin Oncol 1993;11:2101–2111. [PubMed: 8229124]
29. van Baardwijk A, Bosmans G, Boersma L, et al. PET-CT-based autocontouring in non-small-cell lung cancer correlates with pathology and reduces interobserver variability in the delineation of the primary tumor and involved nodal volumes. Int J Radiat Oncol Biol Phys 2007;68:771–778. [PubMed: 17398018]
30. Fox JL, Rengan R, O'Meara W, et al. Does registration of PET and planning CT images decrease interobserver and intraobserver variation in delineating tumor volumes for non-small-cell lung cancer? Int J Radiat Oncol Biol Phys 2005;62:70–75. [PubMed: 15850904]
31. McGarry RC, Papiez L, Williams M, Whitford T, Timmerman RD. Stereotactic body radiation therapy of early-stage non-small-cell lung carcinoma: phase I study. Int J Radiat Oncol Biol Phys 2005;63:1010–105. [PubMed: 16115740]
32. Koong AC, Le QT, Ho A, et al. Phase I study of stereotactic radiosurgery in patients with locally advanced pancreatic cancer. Int J Radiat Oncol Biol Phys 2004;58:1017–1021. [PubMed: 15001240]
33. Schellenberg D, Goodman KA, Lee F, et al. Gemcitabine chemotherapy and single-fraction stereotactic body radiotherapy for locally advanced pancreatic cancer. Int J Radiat Oncol Biol Phys 2008;72:678–686. [PubMed: 18395362]
34. Paulino AC, Johnstone PAS. FDG-PET in radiotherapy treatment planning: Pandora's box? Int J Radiat Oncol Biol Phys 2004;59:4–5. [PubMed: 15093892]
35. Ford EC, Kinahan PE, Hanlon L, et al. Tumor delineation using FDG-PET and FMISO-PET in head and neck and lung cancers: threshold contouring and lesion volumes. Med Phys 2006;33:4280–4288. [PubMed: 17153406]

36. Nestle U, Kremp S, Schaefer-Schuler A, et al. Comparison of different methods for delineation of ^{18}F-FDG PET-positive tissue for target volume definition in radiotherapy of patients with non-small cell lung cancer. J Nucl Med 2005;46:1342–1348. [PubMed: 16085592]
37. Daisne JF, Sibomana M, Bol A, Doumont T, Lonneux M, Gregoire V. Tridimensional automatic segmentation of PET volumes based on measured source-to-background ratios: influence of reconstruction algorithms. Radiother Oncol 2003;69:247–250. [PubMed: 14644483]
38. Black QC, Grills IS, Kestin LL, et al. Defining a radiotherapy target with positron emission tomography. Int J Radiat Oncol Biol Phys 2004;60:1272–1282. [PubMed: 15519800]
39. Ciernik IF, Dizendorf E, Baumert BG, et al. Radiation treatment planning with an integrated positron emission and computer tomography (PET/CT): a feasibility study. Int J Radiat Oncol Biol Phys 2003;57:853–863. [PubMed: 14529793]
40. Erdi YE, Mawlawi O, Larson SM, et al. Segmentation of lung lesion volume by adaptive positron emission tomography image thresholding. Cancer 1997;80(12, suppl):2505–2509. [PubMed: 9406703]
41. Zasadny KR, Kison PV, Francis IR, Wahl RL. FDG-PET determination of metabolically active tumor volume and comparison with CT. Clin Positron Imaging 1998;1:123–129. [PubMed: 14516601]
42. Erdi YE, Rosenzweig K, Erdi AK, et al. Radiotherapy treatment planning for patients with non-small cell lung cancer using positron emission tomography (PET). Radiother Oncol 2002;62:51–60. [PubMed: 11830312]
43. Mah K, Caldwell CB, Ung YC, et al. The impact of ^{18}FDG-PET on target and critical organs in CT-based treatment planning of patients with poorly defined non-small-cell lung carcinoma: a prospective study. Int J Radiat Oncol Biol Phys 2002;52:339–350. [PubMed: 11872279]
44. Bradley J, Thorstad WL, Mutic S, et al. Impact of FDG-PET on radiation therapy volume delineation in non-small-cell lung cancer. Int J Radiat Oncol Biol Phys 2004;59:78–86. [PubMed: 15093902]
45. Scarfone C, Lavely WC, Cmelak AJ, et al. Prospective feasibility trial of radiotherapy target definition for head and neck cancer using 3-dimensional PET and CT imaging. J Nucl Med 2004;45:543–552. [PubMed: 15073248]
46. Ciernik IF, Huser M, Burger C, Davis JB, Szekely G. Automated functional image-guided radiation treatment planning for rectal cancer. Int J Radiat Oncol Biol Phys 2005;62:893–900. [PubMed: 15936575]
47. Paulino AC, Koshy M, Howell R, Schuster D, Davis LW. Comparison of CT- and FDG-PET-defined gross tumor volume in intensity-modulated radiotherapy for head-and-neck cancer. Int J Radiat Oncol Biol Phys 2005;61:1385–1392. [PubMed: 15817341]
48. Aristophanous M, Martel M, Pelizzari C, O'Brien-Penney B. Investigation of a 3D gradient based method for volume segmentation in positron emission tomography for radiation treatment planning [abstract]. Med Phys 2005;32(suppl):1895.
49. Vanuytsel LJ, Vansteenkiste JF, Stroobants SG, et al. The impact of ^{18}F-fluoro-2-deoxy-D-glucose positron emission tomography (FDG-PET) lymph node staging on the radiation treatment volumes in patients with non-small cell lung cancer. Radiother Oncol 2000;55:317–324. [PubMed: 10869746]
50. Wong WL, Hussain K, Chevretton E, et al. Validation and clinical application of computer-combined computed tomography and positron emission tomography with 2-[^{18}F]fluoro-2-deoxy-d-glucose head and neck images. Am J Surg 1996;172:628–632. [PubMed: 8988664]
51. Daisne JF, Duprez T, Weynand B, et al. Tumor volume in pharyngolaryngeal squamous cell carcinoma: comparison at CT, MR imaging, and FDG PET and validation with surgical specimen. Radiology 2004;233:93–100. [PubMed: 15317953]
52. Stroom J, Blaauwgeers H, van Baardwijk A, et al. Feasibility of pathology-correlated lung imaging for accurate target definition of lung tumors. Int J Radiat Oncol Biol Phys 2007;69:267–275. [PubMed: 17707281]
53. Beyer T, Townsend DW, Brun T, et al. A combined PET/CT scanner for clinical oncology. J Nucl Med 2000;41:1369–1379. [PubMed: 10945530]
54. Pan T, Mawlawi O. PET/CT in radiation oncology. Med Phys 2008;35:4955–4966. [PubMed: 19070229]
55. Nehmeh SA, Erdi YE, Ling CC, et al. Effect of respiratory gating on reducing lung motion artifacts in PET imaging of lung cancer. Med Phys 2002;29:366–371. [PubMed: 11929020]

56. Osman MM, Cohade C, Nakamoto Y, Marshall LT, Leal JP, Wahl RL. Clinically significant inaccurate localization of lesions with PET/CT: frequency in 300 patients. J Nucl Med 2003;44:240–243. [PubMed: 12571215]
57. Chi PM, Mawlawi O, Luo D, Liao Z, Macapinlac HA, Pan T. Effects of respiration-averaged computed tomography on positron emission tomography/computed tomography quantification and its potential impact on gross tumor volume delineation. Int J Radiat Oncol Biol Phys 2008;71:890–899. [PubMed: 18514781]
58. Ford EC, Mageras GS, Yorke E, Ling CC. Respiration-correlated spiral CT: a method of measuring respiratory-induced anatomic motion for radiation treatment planning. Med Phys 2003;30:88–97. [PubMed: 12557983]
59. Vedam SS, Keall PJ, Kini VR, Mostafavi H, Shukla HP, Mohan R. Acquiring a four-dimensional computed tomography dataset using an external respiratory signal. Phys Med Biol 2003;48:45–62. [PubMed: 12564500]
60. Nehmeh SA, Erdi YE, Pan T, et al. Four-dimensional (4D) PET/CT imaging of the thorax. Med Phys 2004;31:3179–3186. [PubMed: 15651600]
61. Meirelles GSP, Erdi YE, Nehmeh SA, et al. Deep-inspiration breath-hold PET/ CT: clinical findings with a new technique for detection and characterization of thoracic lesions. J Nucl Med 2007;48:712–719. [PubMed: 17475958]
62. Kawano T, Ohtake E, Inoue T. Deep-inspiration breath-hold PET/CT of lung cancer: maximum standardized uptake value analysis of 108 patients. J Nucl Med 2008;49:1223–1231. [PubMed: 18632812]
63. Arriagada R, Komaki R, Cox JD. Radiation dose escalation in non-small cell carcinoma of the lung. Semin Radiat Oncol 2004;14:287–291. [PubMed: 15558502]
64. Grills IS, Yan D, Martinez AA, Vicini FA, Wong JW, Kestin LL. Potential for reduced toxicity and dose escalation in the treatment of inoperable non-small-cell lung cancer: a comparison of intensity-modulated radiation therapy (IMRT), 3D conformal radiation, and elective nodal irradiation. Int J Radiat Oncol Biol Phys 2003;57:875–890. [PubMed: 14529795]
65. Stevens, C. Lung cancer radiotherapy. In: Palta, J.; Mackie, TR., editors. Intensity-Modulated Radiation Therapy: The State of the Art. Madison, WI: Medical Physics Publishing Corp.; 2003. p. 645
66. Bortfeld T, Jokivarsi K, Goitein M, Kung J, Jiang SB. Effects of intra-fraction motion on IMRT dose delivery: statistical analysis and simulation. Phys Med Biol 2002;47:2203–2220. [PubMed: 12164582]
67. Chui CS, Yorke E, Hong L. The effects of intra-fraction organ motion on the delivery of intensity-modulated field with a multileaf collimator. Med Phys 2003;30:1736–1746. [PubMed: 12906191]
68. Liu HH, Balter P, Tutt T, et al. Assessing respiration-induced tumor motion and internal target volume using four-dimensional computed tomography for radiotherapy of lung cancer. Int J Radiat Oncol Biol Phys 2007;68:531–540. [PubMed: 17398035]
69. Yom SS, Liao Z, Liu HH, et al. Initial evaluation of treatment-related pneumonitis in advanced-stage non-small-cell lung cancer patients treated with concurrent chemotherapy and intensity-modulated radiotherapy. Int J Radiat Oncol Biol Phys 2007;68:94–102. [PubMed: 17321067]
70. Sura S, Gupta V, Yorke E, Jackson A, Amols H, Rosenzweig KE. Intensity-modulated radiation therapy (IMRT) for inoperable non-small cell lung cancer: the Memorial Sloan-Kettering Cancer Center (MSKCC) experience. Radiother Oncol 2008;87:17–23. [PubMed: 18343515]
71. Timmerman RD, Park C, Kavanagh BD. The North American experience with stereotactic body radiation therapy in non-small cell lung cancer. J Thorac Oncol 2007;2(7 suppl 3):S101–S112. [PubMed: 17603304]
72. Papiez L, Timmerman R. Hypofractionation in radiation therapy and its impact. Med Phys 2008;35:112–118. [PubMed: 18293568]
73. Gambhir SS, Czernin J, Schwimmer J, Silverman DH, Coleman RE, Phelps ME. A tabulated summary of the FDG PET literature. J Nucl Med 2001;42(5, suppl):1S–93S. [PubMed: 11483694]
74. Mac Manus MP, Hicks RJ, Ball DL, et al. F-18 fluorodeoxyglucose positron emission tomography staging in radical radiotherapy candidates with nonsmall cell lung carcinoma: powerful correlation with survival and high impact on treatment. Cancer 2001;92:886–895. [PubMed: 11550162]

75. Nestle U, Walter K, Schmidt S, et al. ^{18}F-deoxyglucose positron emission tomography (FDG-PET) for the planning of radiotherapy in lung cancer: high impact in patients with atelectasis. Int J Radiat Oncol Biol Phys 1999;44:593–597. [PubMed: 10348289]
76. Kiffer JD, Berlangieri SU, Scott AM, et al. The contribution of ^{18}F-fluoro-2-deoxy-glucose positron emission tomographic imaging to radiotherapy planning in lung cancer. Lung Cancer 1998;19:167–177. [PubMed: 9631364]
77. Munley MT, Marks LB, Scarfone C, et al. Multimodality nuclear medicine imaging in three-dimensional radiation treatment planning for lung cancer: challenges and prospects. Lung Cancer 1999;23:105–114. [PubMed: 10217614]
78. Bradley JD, Perez CA, Dehdashti F, Siegel BA. Implementing biologic target volumes in radiation treatment planning for non-small cell lung cancer. J Nucl Med 2004;45(suppl 1):96S–101S. [PubMed: 14736840]
79. Nestle U, Kremp S, Grosu A. Practical integration of [^{18}F]-FDG-PET and PET-CT in the planning of radiotherapy for non-small cell lung cancer (NSCLC): the technical basis, ICRU-target volumes, problems, perspectives. Radiother Oncol 2006;81:209–225. [PubMed: 17064802]
80. Caldwell CB, Mah K, Skinner M, Danjoux CE. Can PET provide the 3D extent of tumor motion for individualized internal target volumes? A phantom study of the limitations of CT and the promise of PET. Int J Radiat Oncol Biol Phys 2003;55(5):1381–1393. [PubMed: 12654451]
81. Hoopes DJ, Tann M, Fletcher JW, et al. FDG-PET and stereotactic body radiotherapy (SBRT) for stage I non-small-cell lung cancer. Lung Cancer 2007;56:229–234. [PubMed: 17353064]
82. Videtic GMM, Rice TW, Murthy S, et al. Utility of positron emission tomography compared with mediastinoscopy for delineating involved lymph nodes in stage III lung cancer: insights for radiotherapy planning from a surgical cohort. Int J Radiat Oncol Biol Phys 2008;72:702–706. [PubMed: 18374513]
83. Crippa F, Leutner M, Belli F, et al. Which kinds of lymph node metastases can FDG PET detect? A clinical study in melanoma. J Nucl Med 2000;41(9):1491–1494. [PubMed: 10994727]
84. Garden AS, Morrison WH, Rosenthal DI, Chao KSC, Ang KK. Target coverage for head and neck cancers treated with IMRT: review of clinical experiences. Semin Radiat Oncol 2004;14:103–109. [PubMed: 15095256]
85. Eisbruch A, Ten Haken RK, Kim HM, Marsh LH, Ship JA. Dose, volume, and function relationships in parotid salivary glands following conformal and intensity-modulated irradiation of head and neck cancer. Int J Radiat Oncol Biol Phys 1999;45:577–587. [PubMed: 10524409]
86. Wang D, Schultz CJ, Jursinic PA, et al. Initial experience of FDG-PET/CT guided IMRT of head-and-neck carcinoma. Int J Radiat Oncol Biol Phys 2006;65(1):143–151. [PubMed: 16618577]
87. Nishioka T, Shiga T, Shirato H, et al. Image fusion between ^{18}FDG-PET and MRI/CT for radiotherapy planning of oropharyngeal and nasopharyngeal carcinomas. Int J Radiat Oncol Biol Phys 2002;53:1051–1057. [PubMed: 12095574]
88. Nuyts S, Dirix P, Hermans R, et al. Early experience with a hybrid accelerated radiotherapy schedule for locally advanced head and neck cancer. Head Neck 2007;29(8):720–730. [PubMed: 17315171]
89. Gomez DR, Hoppe BS, Wolden SL, Zhung JE, Patel SG, Kraus DH, et al. Outcomes and prognostic variables in adenoid cystic carcinoma of the head and neck: a recent experience. Int J Radiat Oncol Biol Phys 2008;70:1365–1372. [PubMed: 18029108]
90. Schoenfeld GO, Amdur RJ, Morris CG, Li JG, Hinerman RW, Mendenhall WM. Patterns of failure and toxicity after intensity-modulated radiotherapy for head and neck cancer. Int J Radiat Oncol Biol Phys 2008;71:377–385. [PubMed: 18164838]
91. Cannon DM, Lee NY. Recurrence in region of spared parotid gland after definitive intensity-modulated radiotherapy for head and neck cancer. Int J Radiat Oncol Biol Phys 2008;70:660–665. [PubMed: 18037580]
92. Schechter NR, Gillenwater AM, Byers RM, et al. Can positron emission tomography improve the quality of care for head-and-neck cancer patients? Int J Radiat Oncol Biol Phys 2001;51:4–9. [PubMed: 11516844]
93. Schwartz DL, Ford E, Rajendran J, et al. FDG-PET/CT imaging for preradiotherapy staging of head-and-neck squamous cell carcinoma. Int J Radiat Oncol Biol Phys 2005;61:129–136. [PubMed: 15629603]

94. Sanguineti G, Gunn GB, Endres EJ, Chaljub G, Cheruvu P, Parker B. Patterns of locoregional failure after exclusive IMRT for oropharyngeal carcinoma. Int J Radiat Oncol Biol Phys 2008;72:737–746. [PubMed: 18486356]
95. Schwartz DL, Ford EC, Rajendran J, et al. FDG-PET/CT-guided intensity modulated head and neck radiotherapy: a pilot investigation. Head Neck 2005;27:478–487. [PubMed: 15772953]
96. Steenbakkers RJ, Duppen JC, Fitton I, et al. Reduction of observer variation using matched CT-PET for lung cancer delineation: a three-dimensional analysis. Int J Radiat Oncol Biol Phys 2006;64:435–448. [PubMed: 16198064]
97. Nakamoto Y, Tatsumi M, Hammoud D, Cohade C, Osman MM, Wahl RL. Normal FDG distribution patterns in the head and neck: PET/CT evaluation. Radiology 2005;234:879–885. [PubMed: 15734938]
98. Chen W. Clinical applications of PET in brain tumors. J Nucl Med 2007;48:1468–1481. [PubMed: 17704239]
99. Spence AM, Muzi M, Mankoff DA, O'Sullivan SF, Link JM, Lewellen TK, et al. ^{18}F-FDG PET of gliomas at delayed intervals: improved distinction between tumor and normal gray matter. J Nucl Med 2004;45:1653–1659. [PubMed: 15471829]
100. Grosu AL, Weber WA, Franz M, et al. Reirradiation of recurrent high-grade gliomas using amino acid PET (SPECT)/CT/MRI image fusion to determine gross tumor volume for stereotactic fractionated radiotherapy. Int J Radiat Oncol Biol Phys 2005:63511–63519.
101. Chen W, Cloughesy T, Kamdar N, et al. Imaging proliferation in brain tumors with ^{18}F-FLT PET: comparison with ^{18}F-FDG. J Nucl Med 2005;46:945–952. [PubMed: 15937304]
102. Tralins KS, Douglas JG, Stelzer KJ, et al. Volumetric analysis of ^{18}F-FDG PET in glioblastoma multiforme: prognostic information and possible role in definition of target volumes in radiation dose escalation. J Nucl Med 2002;43:1667–1673. [PubMed: 12468518]
103. Douglas JG, Stelzer KJ, Mankoff DA, et al. [F-18]-fluorodeoxyglucose positron emission tomography for targeting radiation dose escalation for patients with glioblastoma multiforme: clinical outcomes and patterns of failure. Int J Radiat Oncol Biol Phys 2006;64:886–891. [PubMed: 16242251]
104. Jemal A, Siegel R, Ward E, et al. Cancer statistics, 2008. CA Cancer J Clin 2008;58:71–96. [PubMed: 18287387]
105. Hoyer M, Roed H, Sengelov L, et al. Phase-II study on stereotactic radiotherapy of locally advanced pancreatic carcinoma. Radiother Oncol 2005;76:48–53. [PubMed: 15990186]
106. A randomized phase III study of conventional whole breast irradiation (WBI) versus partial breast irradiation (PBI) for women with stage 0, I, or II breast cancer. Radiation Therapy Oncology Group Web site. [August 6, 2009]. Available at: http://www.rtog.org/members/protocols/0413/0413broadcast.html
107. Ford EC, Lavely WC, Frassica DA, et al. Comparison of FDG-PET/CT and CT for delineation of lumpectomy cavity for partial breast irradiation. Int J Radiat Oncol Biol Phys 2008;71:595–602. [PubMed: 18394814]
108. Brown RS, Leung JY, Fisher SJ, Frey KA, Ethier SP, Wahl RL. Intratumoral distribution of tritiated-FDG in breast carcinoma: correlation between glut-1 expression and FDG uptake. J Nucl Med 1996;37:1042–1047. [PubMed: 8683298]
109. van Baardwijk A, Dooms C, van Suylen RJ, et al. The maximum uptake of ^{18}F-deoxyglucose on positron emission tomography scan correlates with survival, hypoxia inducible factor-1a and GLUT-1 in non-small cell lung cancer. Eur J Cancer 2007;43:1392–1398. [PubMed: 17512190]
110. Higashi K, Ueda Y, Yagishita M, et al. FDG PET measurement of the proliferative potential of non-small cell lung cancer. J Nucl Med 2000;41:85–92. [PubMed: 10647609]
111. Sugawara Y, Braun DK, Kison PV, Russo JE, Zasadny KR, Wahl RL. Rapid detection of human infections with fluorine-18 fluorodeoxyglucose and positron emission tomography: preliminary results. Eur J Nucl Med 1998;25:1238–1243. [PubMed: 9724371]
112. Zasadny KR, Tatsumi M, Wahl RL. FDG metabolism and uptake versus blood flow in women with untreated primary breast cancers. Eur J Nucl Med Mol Imaging 2003;30:274–280. [PubMed: 12552346]

113. Vesselle H, Salskov A, Turcotte E, et al. Relationship between non-small cell lung cancer FDG uptake at PET, tumor histology, and ki-67 proliferation index. J Thorac Oncol 2008;3:971–978. [PubMed: 18758298]

114. Yamamoto Y, Nishiyama Y, Ishikawa S, et al. Correlation of ^{18}F-FLT and ^{18}F-FDG uptake on PET with ki-67 immunohistochemistry in non-small cell lung cancer. Eur J Nucl Med Mol Imaging 2007;34:1610–1616. [PubMed: 17530250]

115. Nimmagadda S, Ford EC, Wong JW, Pomper MG. Targeted molecular imaging in oncology: focus on radiation therapy. Semin Radiat Oncol 2008;18:136–148. [PubMed: 18314068]

116. Van de Wiele C, Lahorte C, Oyen W, et al. Nuclear medicine imaging to predict response to radiotherapy: a review. Int J Radiat Oncol Biol Phys 2003;55:5–15. [PubMed: 12504030]

117. Würker M, Herholz K, Voges J, et al. Glucose consumption and methionine uptake in low-grade gliomas after iodine-125 brachytherapy. Eur J Nucl Med 1996;23:583–586. [PubMed: 8698067]

118. Sugiyama M, Sakahara H, Sato K, et al. Evaluation of 3′-deoxy-3′-^{18}F-fluorothymidine for monitoring tumor response to radiotherapy and photodynamic therapy in mice. J Nucl Med 2004;45:1754–1758. [PubMed: 15471845]

119. Glunde K, Ackerstaff E, Mori N, Jacobs MA, Bhujwalla ZM. Choline phospholipid metabolism in cancer: consequences for molecular pharmaceutical interventions. Mol Pharm 2006;3:496–506. [PubMed: 17009848]

120. Lee NY, Mechalakos JG, Nehmeh S, et al. Fluorine-18-labeled fluoromisonidazole positron emission and computed tomography-guided intensity-modulated radiotherapy for head and neck cancer: a feasibility study. Int J Radiat Oncol Biol Phys 2008;70:2–13. [PubMed: 17869020]

121. Nehmeh SA, Lee NY, Schröder H, Squire O, Zanzonico PB, Erdi YE, et al. Reproducibility of intratumor distribution of ^{18}F-fluoromisonidazole in head and neck cancer. Int J Radiat Oncol Biol Phys 2008;70:235–242. [PubMed: 18086391]

122. Lin Z, Mechalakos J, Nehmeh S, Schoder H, Lee N, Humm J, et al. The influence of changes in tumor hypoxia on dose-painting treatment plans based on ^{18}F-FMISO positron emission tomography. Int J Radiat Oncol Biol Phys 2008;70:1219–1228. [PubMed: 18313529]

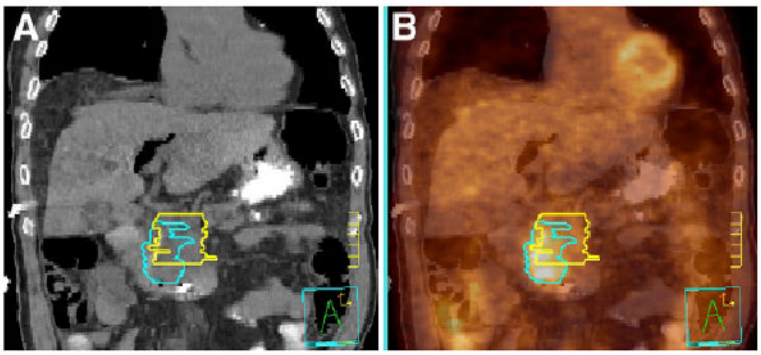

FIGURE 1.
Pancreatic adenocarcinoma delineated on CT alone by radiation oncologist (yellow) and on ^{18}F-FDG PET/ CT by nuclear medicine physician (blue). Images are from coronal cut of patient with CT (A) and ^{18}F-FDG PET/CT image fusion (B). Tick marks are 1 cm.

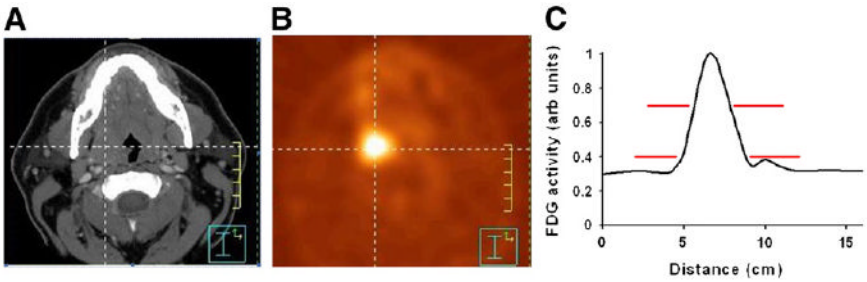

FIGURE 2.

CT (A) and ^{18}F-FDG PET (B) transverse slices for patient with base-of-tongue cancer, and profile plot of ^{18}F-FDG signal along horizontal line (C). Example ^{18}F-FDG signal threshold levels (red lines, C) demonstrate that cutoff levels of 40% and 70% of maximum would result in very different tumor volumes.

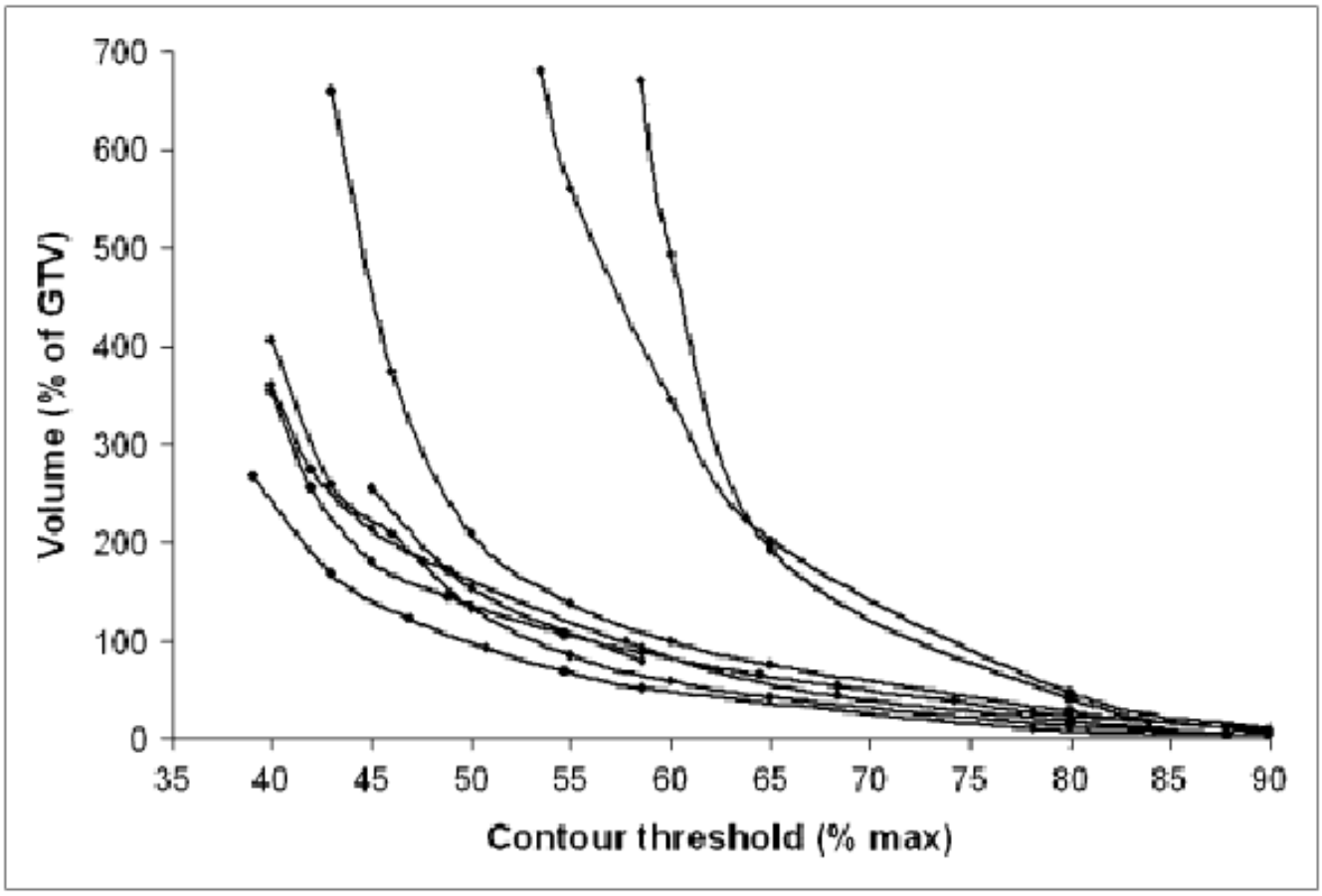

FIGURE 3.
Size of GTV vs. threshold level of ^{18}F-FDG PET signal chosen for automatic contouring. Volumes are plotted as percentage relative to CT-based volume. Data are shown for 8 patients with head and neck cancer.

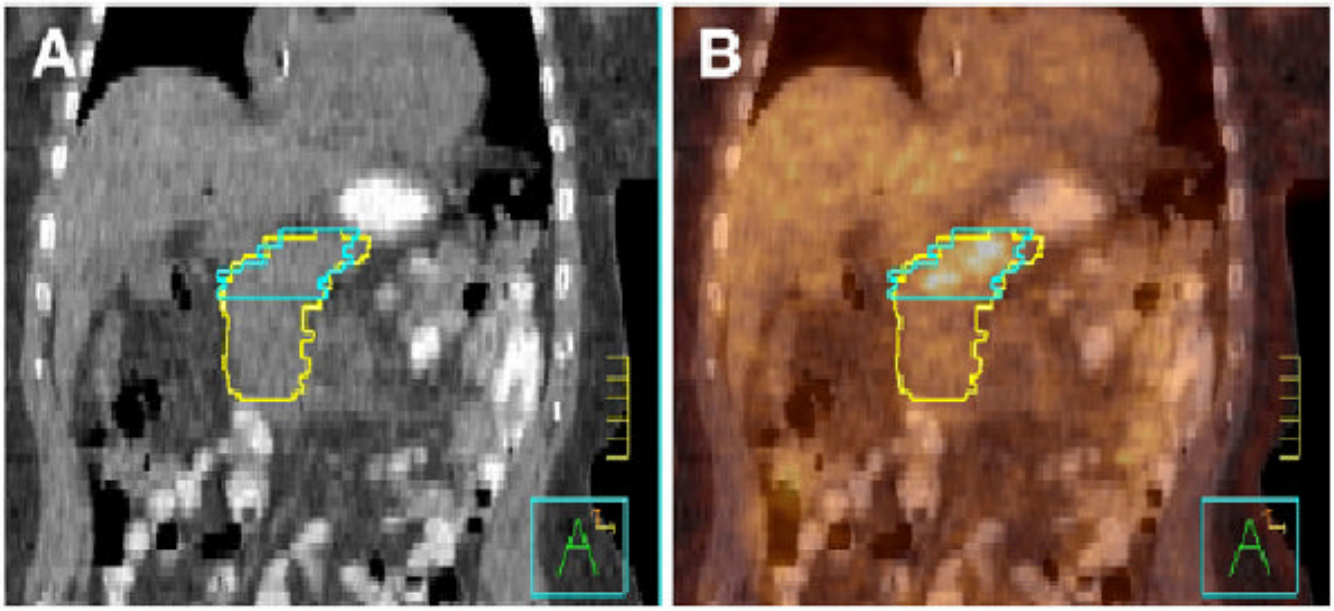

FIGURE 4.

Pancreatic adenocarcinoma delineated on CT alone by radiation oncologist (yellow) and on ^{18}F-FDG PET/ CT by nuclear medicine physician (blue). Images are from coronal cut of patient with CT (A) and ^{18}F-FDG PET/CT image fusion (B). Tick marks are 1 cm.